Electronic supplementary information (ESI)

Directed Holey and Ordered g-$C_3N_{4.5}$ Nanosheets by Hard Template Nanocasting Approach for Sustainable Visible-Light Hydrogen Evolution with Prominent Quantum Efficiency

Bindu Antil,[a] Ravi Ranjan,[b] Chinnakonda S. Gopinath,[b] Sasanka Deka[a,]*

[a]Nanochemistry Laboratory, Department of Chemistry, University of Delhi, North campus, Delhi-110007, India

[b]Catalysis and Inorganic Chemistry Division, National Chemical Laboratory, Dr. Homi Bhabha Road, Pune 411 008, India

*Email: sdeka@chemistry.du.ac.in, ssdeka@gmail.com

Synthesis of SBA-15 Template. The SBA-15 template has been synthesized by following a reported protocol.[1] 4g of the amphiphilic triblock copolymer (P123) was dissolved in 30 ml of deionised water and 120 ml 2M HCl solution. The reaction mixture was then kept for stirring for 5 hours till the complete dissolution of the triblock polymer. To it then added dropwise 9.6 ml of tetraethylorthosilicate (TEOS) under continuous stirring. A gel like suspension was formed which was transferred to Teflon lined autoclave and aged at 40 °C for 24 hours and then finally heated at 150 °C for 24 hours. The white solid product obtained was filtered hot and washed with ethanol and then dried at room temperature. The product obtained was then calcined in air at 550°C for 6 hours in order to decompose the triblock polymer.

Characterization of the Samples.

Powder X-ray diffraction (XRD) profiles were recorded on a Bruker D8 Advance Diffractometer using monochromatized Cu Kα (λ = 1.54 Å) radiation source. The small angle X-ray scattering experiments were carried on a Xuess SAXS/WAXS system (Model C HP100 fm) employed with a micro focused sealed tube with Cu anode (X-ray source). The diffractograms were recorded in

a 2θ range of 1.3° to 4 ° with a 2θ step size of 0.02°. Nitrogen adsorption and desorption measurements were recorded on a Quantachrome (Model ASI-CI-11) BET surface area analyzer. Prior to adsorption analysis, the samples were outgassed at 150 °C for 6h. The specific surface area and size of the pores were determined using Brunauer –Emmett-Teller (BET) method and Barrett-Joyner-Halenda (BJH) method respectively. FT-IR spectra were recorded on a Spectrum RXI-Mid IR (Perkin Elmer) FT-IR spectrometer in the wavelength range of 400-4000 cm^{-1} using standard KBr disk method. In order to know the thermal stability of the samples, thermogravimetric measurements under nitrogen flow (flow rate of 20 cm^3/ min) were performed using Mettler Toledo TGA 1 instrument operated in a temperature range of 5-800 °C with a heating rate of 5°/ min. The morphology of the synthesized materials were examined using a Thermo-Scientific Talos Cryo-Transmission Electron Microscope (Cryo-TEM). In order to obtain the TEM and HRTEM images of the sample, a drop of dilute solution of finely dispersed material was drop casted onto carbon coated Cu grid substrate and finally images were recorded. To get the knowledge of free electrons on the surface of the materials, Bruker Model EMX MicroX spectrometer was used to perform Electron Paramagnetic Resonance (EPR) measurements. To gain insight of the chemical bonding and the elemental composition, X-ray Photoelectron Spectroscopy (XPS) measurements were performed on a Prevac MX650 XPS system employed with Scienta monochromator (Al Kα anode, 1486.6 eV) and Scienta R3000HP differentially pumped analyzer. C1s peak at 284.4 eV was taken as a reference for all other binding energies. XPS valence band spectroscopy was also performed in order to obtain the valence band-edge position. CHN analysis of the samples were determined using Elementar Analysensysteme (Model Vario Micro cube, Germany) CHNS analyzer. UV-Vis spectrophotometer (Perkin Elmer LAMDA 35) was used to collect UV-Vis absorption spectra in the range of 300-900 cm^{-1} using IPA as the reference standard. Cary Eclipse Fluorescence spectrophotometer was used to perform room temperature Photoluminescence (PL) spectroscopy using 350 nm as the excitation wavelength. Time-Resolved Photoluminescence (TRPL) spectrophotometer (Horiba Yvon) was used to determine the average lifetime of the samples using excitation wavelength of 370 nm. To determine the absolute band-edge positions relative to the normal hydrogen electrode (NHE) at pH 7, 10 μL of sample ink was deposited over glassy carbon electrodes (GCE). Prior deposition, the ink preparation was done as follows: 10 mg of the M3AT sample was dispersed in 1 mL IPA and to it added 10 μL of Nafion binder and the

resultant mixture was ultrasonicated for 30 min to obtain a well dispersed sample ink. Dynamic impedance method was opted to obtain the flat band edge potential.

Photocurrent and electrochemical impedance spectroscopy (EIS) measurements. The preparation of working electrodes was done as follows: As-prepared samples 10 mg (M3AT, B3AT) were initially dissolved in 0.5 ml DMF and 20 µL Nafion binder and the mixture was sonicated for 30 min. The slurry was then deposited onto substrate of 1 x 1 cm^2 FTO glass. Before the deposition, the FTO substrate was thoroughly cleaned using a mixture of acetone, ethanol and water by sonication for 10 min at least three times. The electrodes were then dried at 80 ˚C for 1 hour and then sintered at 150 ˚C for 1 h to improve adhesion. The photoelectrochemical measurements were conducted using 0.5 M Na_2SO_4 solution in a three-electrode system where the FTO electrode deposited with the carbon nitride samples was used a working electrode, Pt sheet was used as the counter-electrode and Ag/AgCl was used as the reference electrode. The interval of light-on and light-off is 25 s. The photocurrent responses were measured without any bias voltage. The photocurrent response plots and EIS plots were measured on an electrochemical workstation (CHI660E, USA).

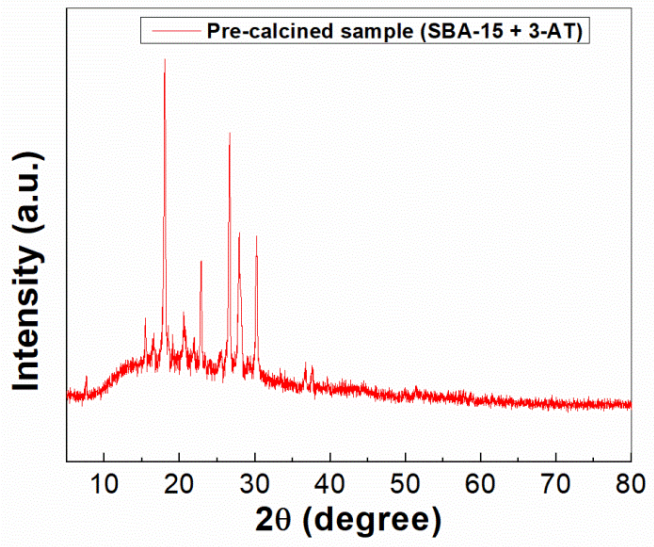

Fig. S1. Powder XRD pattern of the aliquot sample collected after refluxing step and before the calcination step.

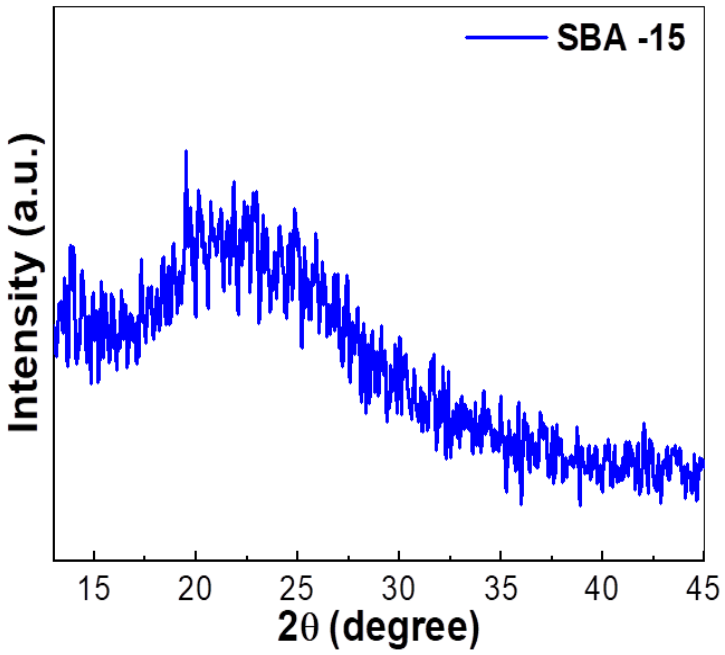

Fig. S2. Wide angle XRD pattern of the as-prepared SBA-15 silica template.

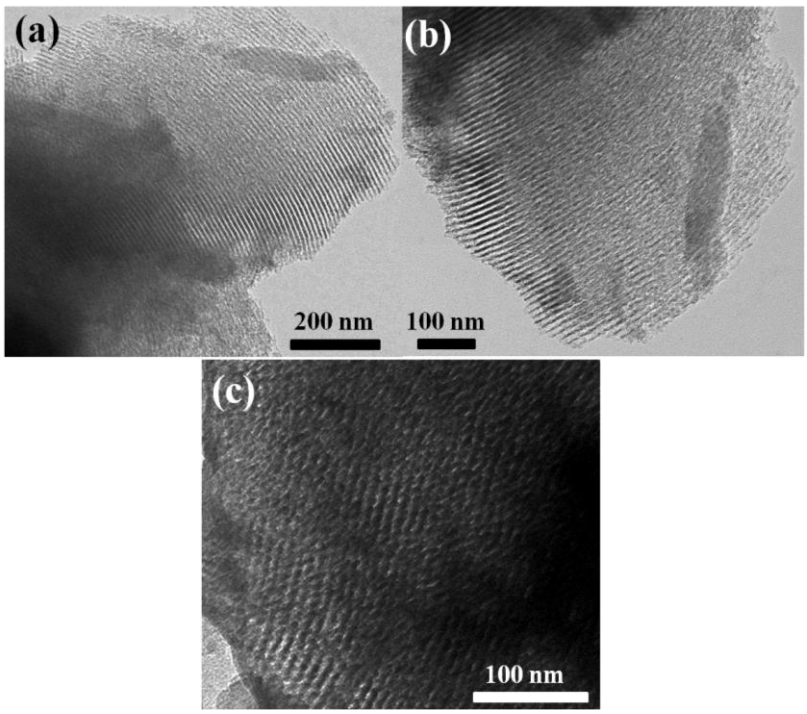

Fig. S3. (a-c) TEM images of the M3AT sample at different magnifications showing mesoporous structure.

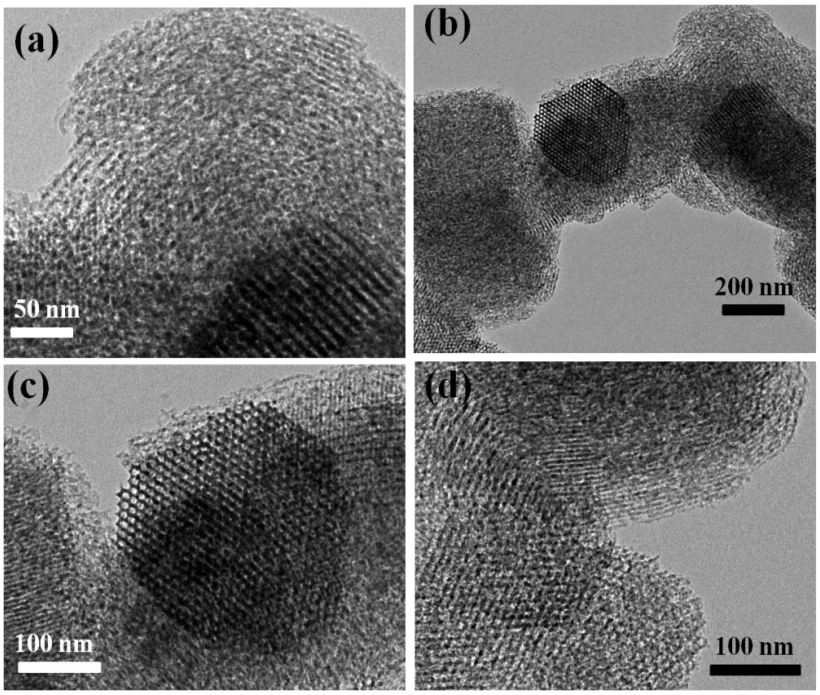

Fig. S4. (a-d) TEM images of as-prepared parent SBA-15 silica template at different magnification scale.

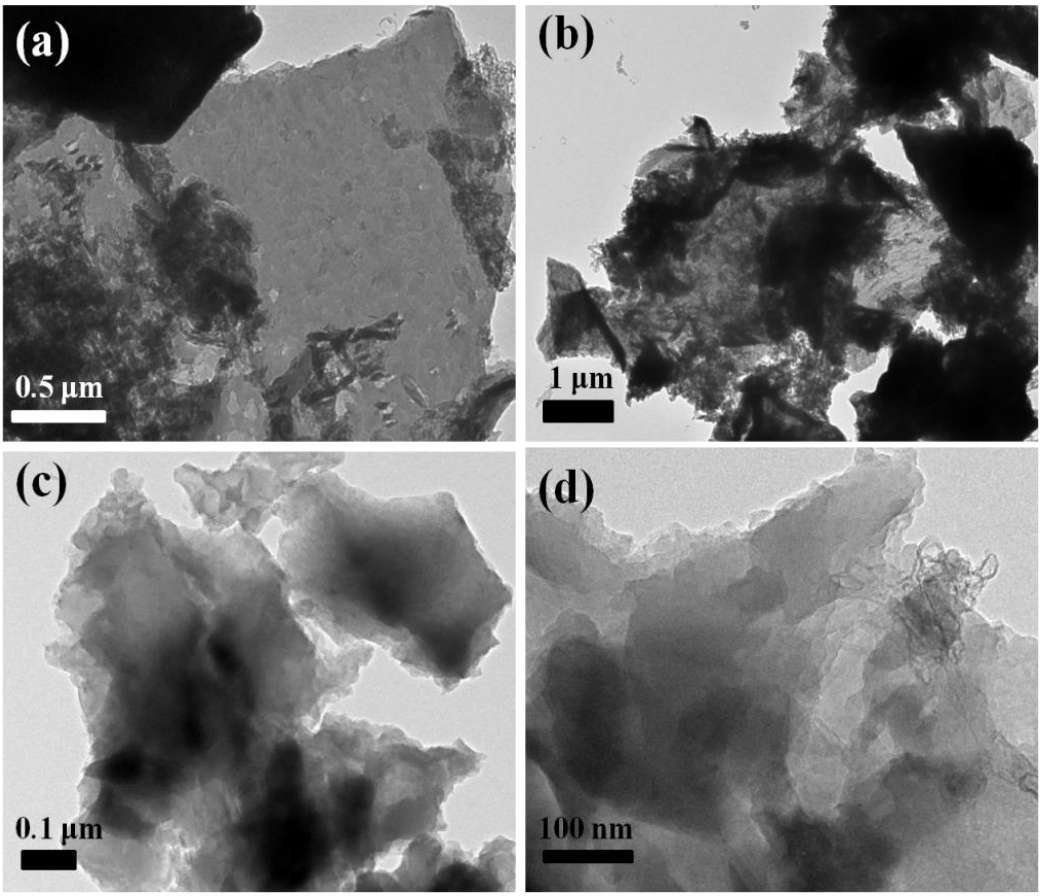

Fig. S5. (a-d) TEM images of as-prepared bulk (B3AT) sample.

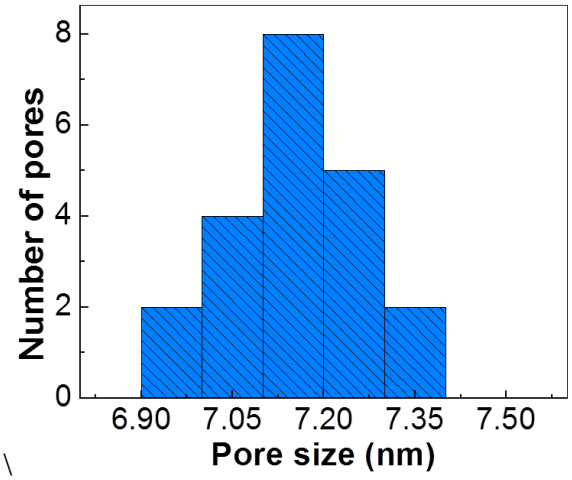

Fig. S6. Plot of number of pores versus pore size (nm) to determine the average size of the mesopores.

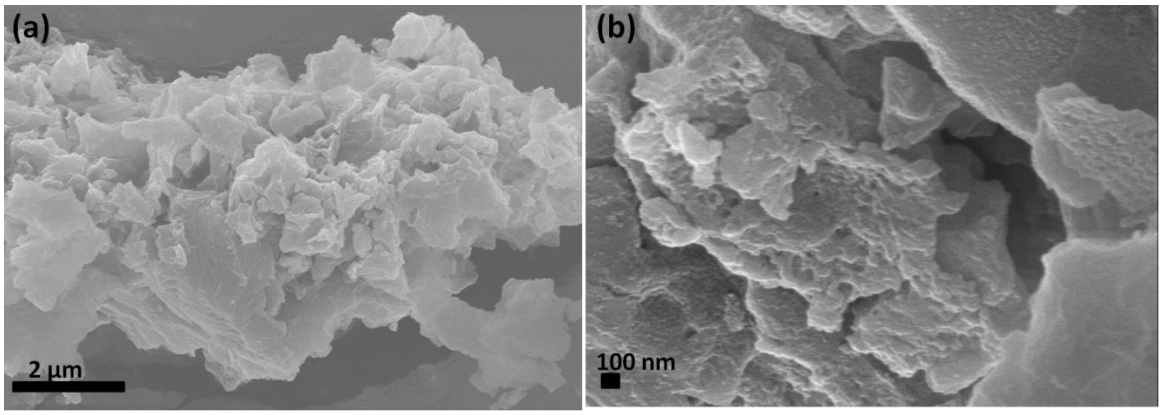

Fig. S7. SEM images of M3AT sample at two different magnifications.

Table S1. Structural parameters of Mesoporous carbon nitride M3AT obtained using nanocasting technique with SBA-15 as template (SBA-15 included for comparison).

Sample	S_{BET} (m^2g^{-1})	Pore volume [a](cm^3 g^{-1})	Pore size[b] (nm)	Pore size from TEM (nm)	d_{100}[c] (nm)	a_o[d] (nm)	wall thickness[e] (nm)
SBA-15	102	0.31	7.5	7.5	5.9	20.43	2.47
M3AT	382	0.789	7.2	7.15	5.5	19.02	1.05

[a]Evaluated at P/P_o= 0.99 , where P is the equilibrium pressure and P_o is the saturation pressure of nitrogen at 77K. [b]Determined using BJH method from the centre of the pore size distribution curve obtained from the adsorption branch. [c]d (100) spacing of the characteristic reflection.

[d]Calculated using the equation[2] $a_o = 2d_{100}\sqrt{3}$. S1

[e]Determined using the following equations: $w_d = c\ d \left(\frac{\rho V_p}{1+\rho V_p}\right)^{1/2}$ S2

where:

w_d is the primary mesopore diameter.

d is the XRD (100) reflection plane spacing.

c is a constant characteristic of the pore geometry and equals to 1.213 for circular as well as hexagonal pores.

ρ is pore wall density and assumed to be 2.2 $cm^3\ g^{-1}$

The pore wall thickness b_d is determined further using the equation :

$$b_d = \left(\frac{2}{\sqrt{3}}\right) d_{100} - \frac{w_d}{1.050} \qquad \text{S3}$$

Table S2. Comaprison of Structural parameters of Mesoporous carbon nitride M3AT obtained with earlier reports.

SI. No.	**2D Mesoporous Materials**	**Surface Area (m^2g^{-1})**	**Pore Volume ($cm^3\ g^{-1}$)**	**Pore size (nm)**	**References**
1.	C_3N_4	239.17	0.59	4.89	3
2.	MCN-1-150	650	0.89	6.40	4
3.	MCN-8	298	0.66	5.8	5
4.	**M3AT**	**382**	**0.79**	**7.2**	**This work**

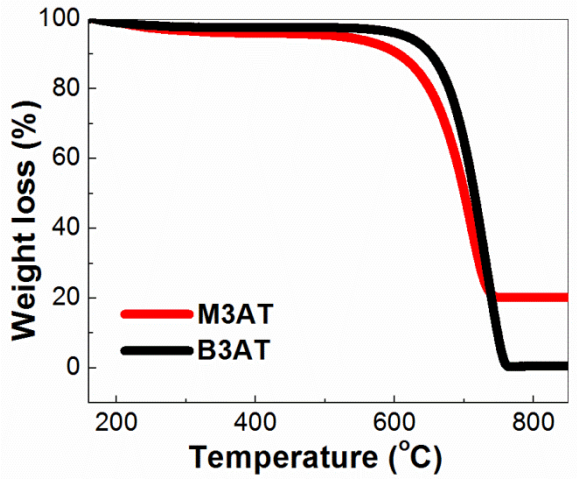

Fig. S8. Thermogravimetric (TGA) curves of both the bulk B3AT and as-synthesized M3AT samples conducted in nitrogen atmosphere.

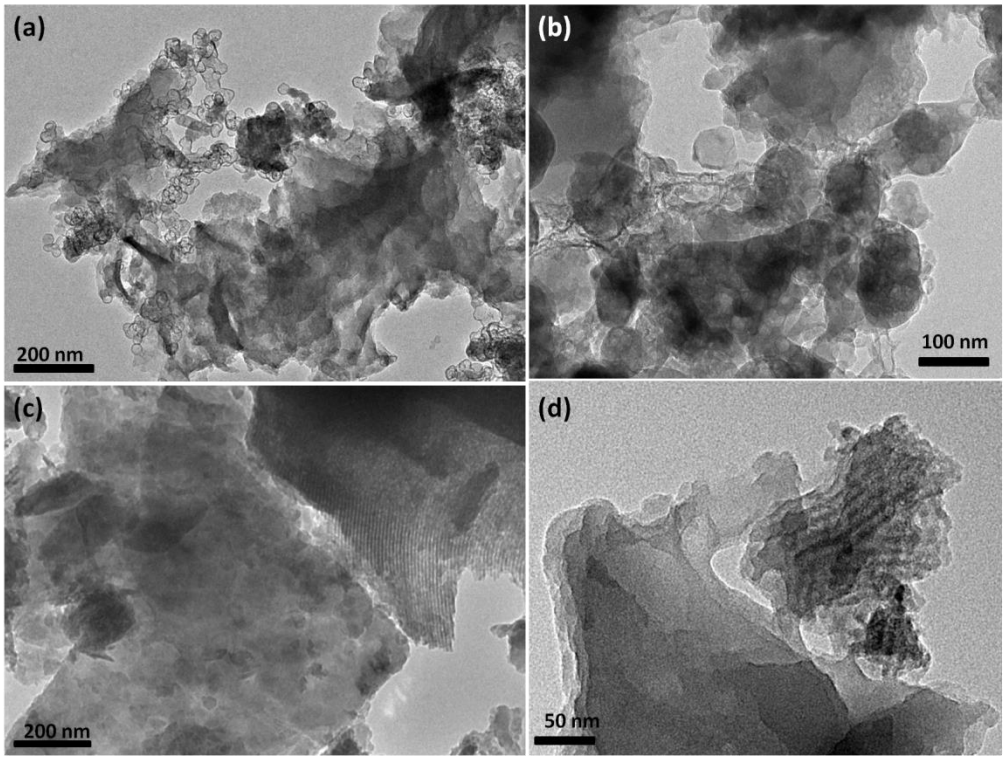

Fig. S9. TEM images of the sample prepared using (a,b) 3g 3-AT +0.5 g SBA-15 at similar reaction conditions as for M3AT. (c,d) 1.5 g 3-AT +1g SBA-15 at similar reaction conditions as for M3AT.

Table S3. Corresponding CHN analysis of M3AT sample to analyze the elemental composition.

Sample code	**C [%]**	**N [%]**	**H [%]**	**C/N ratio**	**Stoichiometry**
M3AT	30.12	52.47	2.349	0.66	$C_3N_{4.5}$
B3AT	32.20	50.02	2.87	0.749	C_3N_4

Calculations of average lifetime:

The average lifetime (τ_a) can be determined using the following equation:

$$\tau_a = \frac{A_1\tau_1^2+A_2\tau_2^2+A_3\tau_3^2}{A_1\tau_1+A_2\tau_2+A_3\tau_3} \quad \text{S4}$$

where τ_1, τ_2 and τ_3 are lifetime components correspond to the initially fast and the followed two slow decays, respectively, and A_1, A_2 and A_3 are the amplitudes of the components, respectively.

Table S4. The decay lifetimes and the average lifetime of photoexcited charge carriers in B3AT and M3AT photocatalysts are listed below:

Sample	Decay life time (ns)			Avg. life time (ns)
	$\boldsymbol{\tau_1}$	$\boldsymbol{\tau_2}$	$\boldsymbol{\tau_3}$	
B3AT	2.2	9.2	0.24	**6.53**
M3AT	2.62	0.4	12.2	**7.72**

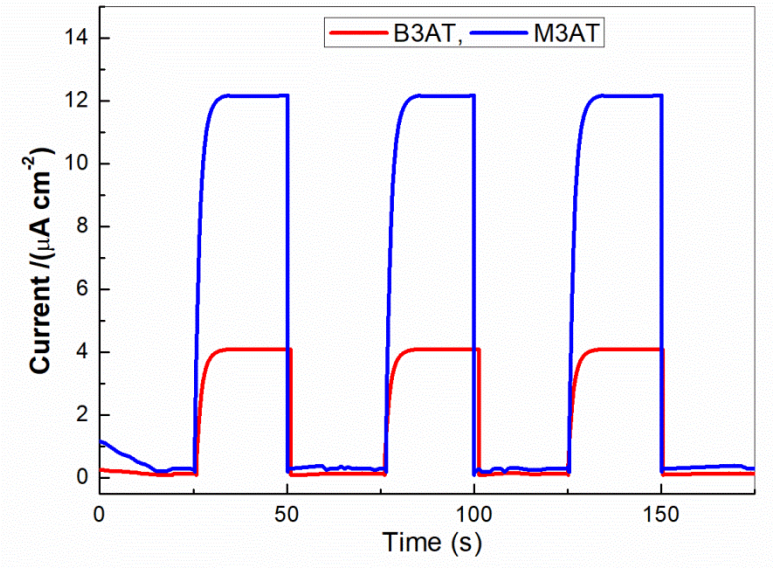

Fig. S10. Photocurrent response of M3AT and B3AT samples.

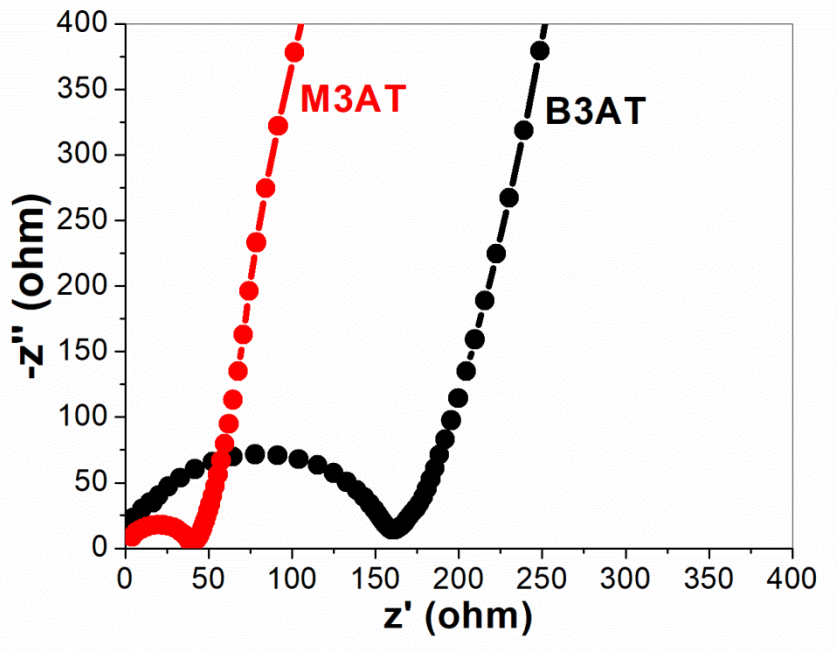

Fig. S11. EIS spectra of M3AT and B3AT

Calculations:

Photocatalytic Reaction

1. **Number of H_2 molecule produced from M3AT using 3 wt% Pt**

Volume of gas liberated in reaction = 10 ml = 0.01 L

Form std. gas equation PV= nRT

n = 0.01 L x 1 atm / 0.082 L.atm mol^{-1} K^{-1} x 298 K

The corresponding amount of hydrogen in moles = 0.000409 moles h^{-1} = 8180 μmol $h^{-1}g^{-1}$

1 mole gas = 6.023 x 10^{23} molecules

0.000409 moles will have = 6.023x 10^{23} x 0.000409

H_2 molecule (*per* cm^2 *per s*) = (6.023 x 10^{23} x 0.000409) / (31.4 x 60 min x 60 s)

= **2.18 x 10^{15}**

H_2 molecule (*per s*) = (6.023 x 10^{23} x 0.000409) / (60 min x 60 s)

= **6.84 x 10^{16}**

2. **Number of H_2 molecule produced from M3AT (no Pt)**

Volume of gas liberated in reaction = 5.1 ml = 0.0051 L

Form std. gas equation PV= nRT

n = 0.0051 L x 1 atm / 0.082 L.atm mol^{-1} K^{-1} x 298 K

The corresponding amount of hydrogen in moles = 0.0002087 moles h^{-1} = 4170 μmol $h^{-1}g^{-1}$

1 mole gas = 6.023 x 10^{23} molecules

0.0002084 moles will have = 6.023x 10^{23} x 0.0002084

H_2 molecule (*per cm^2 per s*) = (6.023 x 10^{23} x 0.0002084) / (31.4 x 60 min x 60 s)

= **1.12 x 10^{15}**

H_2 molecule (*per s*) = (6.023 x 10^{23} x 0.0002084) / (60 min x 60 s)

= **3.49 x 10^{16}**

3. **For Bulk sample (B3AT)**

Volume of gas liberated in reaction = 1.2 ml = 0.0012 L

Form std. gas equation PV= nRT

n = 0.0012 L x 1 atm / 0.082 L.atm mol^{-1} K^{-1} x 298 K

The corresponding amount of hydrogen in moles = 0.00004904 moles h^{-1}

1 mole gas = 6.023 x 10^{23} molecules

0.0000490 moles will have = 6.023x 10^{23} x 0.0000490

H_2 molecule (*per cm^2 per s*) = (6.023 x 10^{23} x 0.0000490) / (31.4 x 60 min x 60 s)

= **2.61 x 10^{14}**

H_2 molecule (*per s*) = (6.023 x 10^{23} x 0.0000490) / (60 min x 60 s)

= **8.20 x 10^{15}**

Apparent Quantum Efficiency (AQE):

$$AQE = \frac{2.nH_2}{(IA\lambda)/(hc)}\ x\ 100\ (\%) \qquad \text{S5}$$

Where nH_2 is the number of H_2 molecule produced per second, *I* is the incident solar irradiance (W/cm^2) over the irradiated area *A* (cm^2), λ is the wavelength of the present study (nm), *h* Planck's constant and *c* is the speed of light.

I = 52500 lux = 0.00768 W/cm^2

A = 31.41 cm^2

1 photon = $\frac{hc}{\lambda}$ =6.626 x10^{-34} x 3 x10^8 / (λ x 10^{-9})

$$AQE = \frac{2\ x\ nH_2}{(0.00768\ x\ 31.41\ x\ \boldsymbol{\lambda}\ x\ 10^{-9})/(6.626\ x\ 10^{-34}\ x\ 3\ x\ 10^{8})} \left(\frac{s^{-1}}{(\frac{W}{cm2}.cm2.m)/(J.s.m.s^{-1})} \right) x\ 100\%$$

Table S5. The apparent quantum efficiency of B3AT, and M3AT samples calculated at all wavelengths (10 nm intervals) till 420 nm from band gap absorption:

SI. N.	Wavelength (λ value in above equation S5)	AQE (%)(bulk B3AT)	AQE (%)(without Pt)	AQE (%) (with Pt)
1.	420	3.25	13.84	27.14
2.	430	3.17	13.53	26.51
3.	440	3.11	13.22	25.90
4.	450	3.04	12.92	25.33
5.	460	2.97	12.64	24.78
6.	470	2.91	11.95	24.25
7.	480	2.85	11.70	23.75

8.	490	2.79	11.46	23.26
9.	500	2.73	11.23	22.80
10.	510	2.68	11.01	22.35

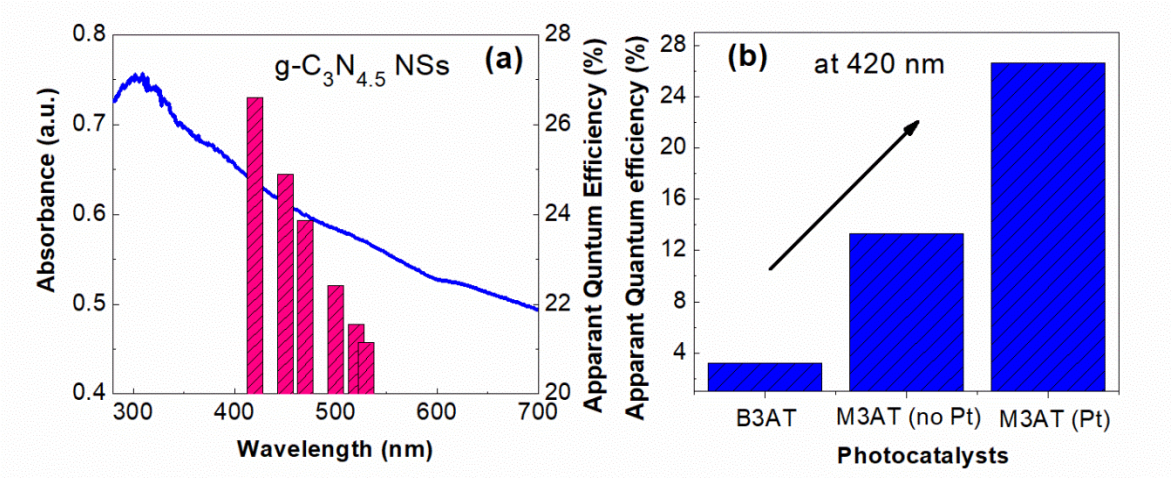

Fig. S12. (a) Apparent quantum efficiency of as-synthesized g-$C_3N_{4.5}$ NSs at different wavelengths, (b) Apparent quantum efficiency vs. different photocatalysts conditions.

Table S6. Comparison of photocatalytic activity of present mesoporous carbon nitride sample with other nanostructured semiconductor photocatalysts.

Sl. No.	**Photocatalyst**	**Amount of photocatalyst and co-catalyst**	**Sacrificial agent**	**Photocatalytic Activity (mmol h^{-1} g^{-1})**	**Apparent Quantum Efficiency (%)**	**Reference No.**
1.	**Mesoporous g-$C_3N_{4.5}$**	**50 mg + 3 wt % Pt**	**20 % vol TEOA**	**8.18**	**27.14 % at 420 nm**	**This work**
		50 mg + without Pt		**4.17**	**13.84 % at 420 nm**	
2.	MCN-8	100 mg + 3wt % Pt	10% vol TEOA	2.6	_	6

3	Holey Graphitic carbon nitride	10 mg + 3wt % Pt	7% vol TEOA	8.2	_	7
4.	Mesoporous carbon nitride	100 mg +3 wt % Pt	10% vol TEOA	0.3	0.21 % at 405 nm	8
5.	Mesoporous carbon nitride	30 mg + 3wt % Pt	10% vol TEOA	1.16	7.7% at 420 nm	9
6.	Onion –ring like porous g-C_3N_4	10 mg + 3 wt % Pt	10% vol TEOA	1.90	-	10
7.	g-C_3N_4	100 mg + 3wt % Pt	10% vol TEOA	2.36	~ 0.1 % at 420-460 nm	11
8.	Post-Calcined Carbon Nitride Nanosheets	50 mg + 2 wt % of Pt	10% vol TEOA	5.2	21.3% at 420 nm	12
9.	P and Na codoped carbon nitride	50 mg + 1 wt % of Pt	20% vol TEOA	2.03	6.79% at 420 nm	13
10.	$Cu_3Nb_{0.9}V_{0.1}S_4$	300 mg + $RuCl_3$	Na_2S + K_2SO_3	1.09	-	14
11.	$Cd_{0.5}Zn_{0.5}S$ QDs/onion like carbon matrix	100 mg	Na_2S + Na_2SO_3	2.018	-	15
12.	FeP/ g-C_3N_4	60 mg + FeP	10% vol. TEOA	0.177	1.57 % at 420 nm	16
13.	Rh_xP/g-C_3N_4	50 mg + Rh_xP	20% vol. TEOA	3.055	18.4 % at 420 nm	17

14.	Ultrathin MOF NSs/ 12 wt% loading of Single Pt Atoms	5 mg + 15 wt% Pt	0.1 M ascorbic acid	11.3	-	18
15.	CeO_2/N,S-C HN	10 mg	8 % vol TEOA	0.55	-	19
16.	CdS/ZnS	50 mg	Na_2S + Na_2SO_3	0.83	-	20
17.	CoNi-$ZnIn_2S_4$	30 mg+ CoNi	0.1 M ascorbic acid	3.336	-	21
18.	Pt/$BaTiO_3$:Rh	100 mg + Pt	10 % aq. MeOH	0.308	-	22
19.	$CsPbBr_{3-x}I_x$/Pt	200 + Pt	Aq. HBr	1.12	2.15% at 450 nm	23
20.	CdS/15wt% VN	40 mg + 15wt% VN	10 % vol. Lactic acid	6.24	5.3 % at 420 nm	24
21.	$CuInS_2$ Nanododecahedrons	10 mg	Na_2S + Na_2SO_3	1.33	-	25
22.	$MnIn_2S_4$	15 mg + 5 wt% $CoSeO_3$	Na_2S + Na_2SO_3	0.319	3.77 at 420 nm	26
23.	Co-O cluster based coordination polymer	4 mg + 4 mg $Ru(bpy)_3Cl_2$	10 % aq. DMF	1.778	-	27
24.	COP-TF@CNi_2P	9 mg	Na_2S + Na_2SO_3	2.5	1.4 % at 500 nm	28
25.	c-CdS/ h-CdS	50 mg	Na_2S + Na_2SO_3	1.789	-	29

27.	g-$C_3N_{4.8}$ nanosheets	50 mg	20% TEOA	2.62	8.5% at 427 nm	30
28.	C_3N_4/CoP	100 mg + CoP (0.25 wt%)	TEOA	0.474	-	31
29.	g-C_3N_4/CoP	50 mg + CoP (3 wt% Co)	TEOA	1.924	12.4% at 420 nm	32

M3AT sample was finely deposited over glass slide as shown above and was used to check the process of hydrogen generation.

Fig. S13. M3AT sample was finely deposited over glass slide as shown above and was used to check the process of hydrogen evolution as shown in an attached supporting video.

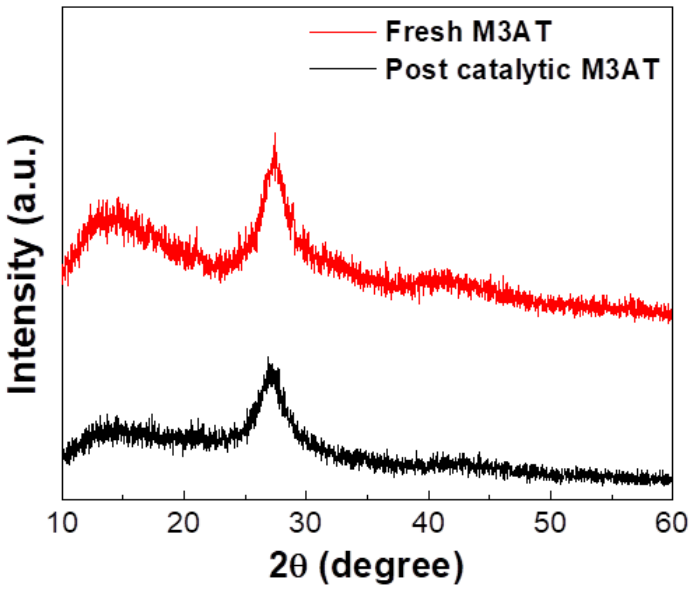

Fig. S14. Comparison of powder XRD patterns of fresh M3AT sample and post-catalytic M3AT sample.

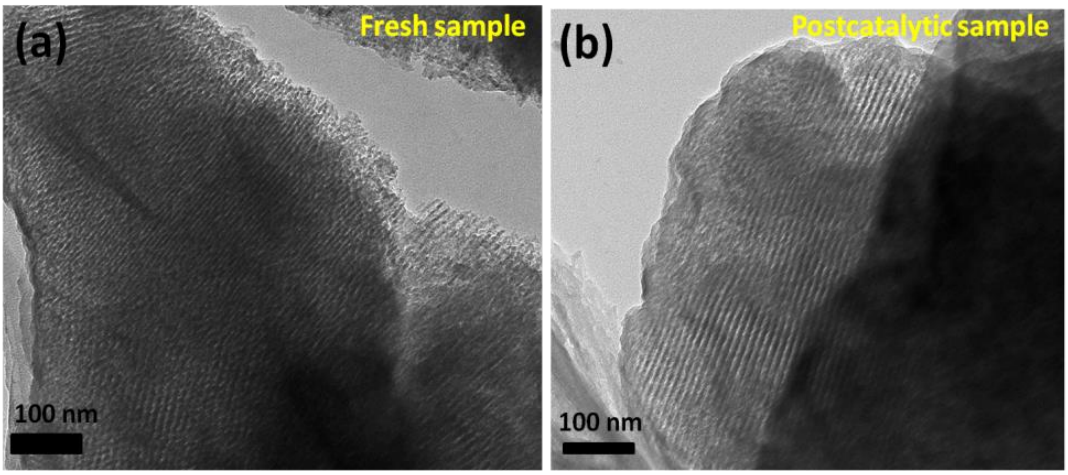

Fig. S15. (a,b) Comparison of HRTEM images of Fresh M3AT sample with the post-catalytic sample.

Supporting References

1. M. Hartmann, A. Vinu. *Langmuir* 2002, **18**, 8010.
2. M. Kruk, M. Jaroniec, Y. Sakamoto, O. Terasaki, R. Ryoo, C. H. Ko. *J. Phys. Chem. B*, 2000, **104**, 292.
3. Y. S. Jun, W. H. Hong, M. Antonietti, A. Thomas. *Adv. Mater.*, 2009, **21**, 4270.

4. A. Vinu. *Adv. Funct. Mater.*, 2008, **18**, 816.
5. S. N. Talapaneni, G. P. Mane, A. Mano, C. Anand, D. S. Dhawale, T. Mori, A. Vinu, *ChemSusChem*, 2012, **5**, 700.
6. G. P. Mane, S. N. Talapaneni, K. S. Lakhi, H. Ilbeygi, U. Ravon, K. Al-Bahily, T. Mori, D. H. Park, A. Vinu, *Angew. Chem. Int. Ed.*, 2017, **56**, 8481.
7. Q. Liang, Z. Li, Z. H. Huang, F. Kang, Q. H. Yang, *Adv. Funct. Mat.*, 2015, **25**, 6885.
8. S. N. Talapaneni, G. P. Mane, D. H. Park, K. S. Lakhi, K. Ramadass, S. Joseph, W. M. Skinner, U. Ravon, K. Al-Bahily, A. Vinu, *J. Mater. Chem. A*, 2017, **5**, 18183.
9. S. Sun, X. Gou, S. Tao, J. Cui, J. Li, Q. Yang, S. Liang, Z. Yang, *Mater. Chem. Front.*, 2019, **3**, 597.
10. L. Cui, J. Song, A. F. McGuire, S. Kang, X. Fang, J. Wang, C. Yin, X. Li, Y. Wang, B. Cui, *ACS Nano*, 2018, **12**, 5551.
11. X. Wang, K. Maeda, A. Thomas, K. Takanabe, G. Xin, J. M. Carlsson, K. Domen, M. Antonietti, *Nat. Mater.*, 2009, **8**, 76.
12. M. R. Gholipour, F. Béland, T. O. Do, *ACS Sustainable Chem. Eng.*, 2016, **5**, 213.
13. Wang, C. Wang, W. Wang, H. Fan, N. Zhao, J. Ma, M. Zhang, A. Yadav, *ACS Appl. Mater. Interfaces*, 2020, **12**, 5234.
14. S. Ikeda, N. Aono, A. Iwase, H. Kobayashi, A. Kudo, *ChemSusChem*, 2019, **12**, 1977.
15. X. Zhou, X. Wang, X. Feng, K. Zhang, X. Peng, H. Wang, C. Liu, Y. Han, H. Wang, Q. Li, *ACS Appl. Mater. Interfaces*, 2017, **9**, 22560.
16. D. Zeng, T. Zhou, W. J. Ong, M. Wu, X. Duan, W. Xu, Y. Chen, Y. A. Zhu, D. L. Peng, *ACS Appl. Mater. Interfaces*, 2019, **11**, 5651.
17. H. Dong, M. Xiao, S. Yu, H. Wu, Y. Wang, J. Sun, G. Chen, C. Li, *ACS Catal.*, 2019, **10**, 458.
18. Q. Zuo, T. Liu, C. Chen, Y. Ji, X. Gong, Y. Mai, Y. Zhou, *Angew. Chem. Int. Ed.*, 2019, **58**, 10198.
19. J. Hao, W. Zhan, L. Sun, G. Zhuang, X. Wang, X. Han, *Inorg. Chem.*, 2019, **59**, 937.
20. J. Kundu, B. K. Satpathy, D. Pradhan, *Ind. Eng. Chem. Res.*, 2019, **58**, 22709.
21. Z. Li, X. Wang, W. Tian, A. Meng, L. Yang, *ACS Sustainable Chem. Eng.*, 2019, **7**, 20190.
22. K. Maeda, *ACS Appl. Mater. Interfaces*, 2014, **6**, 2167.

23. Z. Guan, Y. Wu, P. Wang, Q. Zhang, Z. Wang, Z. Zheng, Y. Liu, Y. Dai, M. H. Whangbo, B. Huang, *Appl. Catal. B Environ.*, 2019, **245**, 522.
24. L. Tian, S. Min, F. Wang, Z. Zhang, *J. Phys. Chem. C*, 2019, **123**, 28640.
25. Y. Li, J. Liu, X. Li, X. Wan, R. Pan, H. Rong, J. Liu, W. Chen, J. Zhang *ACS Appl. Mater. Interfaces* 2019, **11**, 27170.
26. H. Liang, T. Feng, S; Tan, K. Zhao, W. Wang, B. Dong, L. Cao, *Chem. Commun.* 2019, **55**, 15061.
27. M.J. Wei, J.H. Zhang, W.M. Liao, Z.W. Wei, M. Pan, C.Y. Su, *J. Photochem. Photobiol. A* 2020, **387**, 112137.
28. Y. Liu, Z. Xiang, *ACS Appl. Mater. Interfaces* 2019, **11**, 41313.
29. W. Zhong, X. Wu, P. Wang, J. Fan, H. Yu, *ACS Sustainable Chem. Eng.* 2019, **8**, 543.
30. B. Antil, L. Kumar, K.P. Reddy, C.S. Gopinath, S. Deka, *ACS Sustainable Chem. Eng.* 2019, **7**, 9428.
31. S. S. Yi, J. M. Yan, B. R. Wulan, S. J. Li, K. H. Liu, Q. Jiang, *Appl. Catal. B* 2017, **200**, 477.
32. C. Li, Y. Du, D. Wang, S. Yin, W. Tu, Z. Chen, M. Kraft, G. Chen, R. Xu, *Adv. Funct. Mater.* 2017, **27**, 1604328.

***